ELSEVIER

Physica A 211 (1994) 57–83

PHYSICA A

A method for studying stability domains in physical models

Jason A.C. Gallas [1]

Höchstleistungsrechenzentrum, Forschungszentrum Jülich, D-52425 Jülich, Germany

Received 3 March 1994

Abstract

We present a method for investigating the simultaneous movement of all zeros of equations of motions defined by discrete mappings. The method is used to show that knowledge of the interplay of all zeros is of fundamental importance for establishing periodicities and relative stability properties of the various possible physical solutions. The method is also used (i) to show that the *Frontière* set of Fatou is defined primarily by *zeros* of functions leading to an entire *invariant limiting function* which underlies every dynamical system, (ii) to identify cyclotomic polynomials as components of the limiting function obtained for a parameter value supporting a particular superstable orbit of the quadratic map, (iii) to describe highly symmetric periodic cycles embedded in these components, and (iv) to provide an unified picture about which mathematical objects form basin boundaries of dynamical systems in general: the closure of all zeros not belonging to "stable" orbits.

1. Introduction

The purpose of this paper is to present a method to study the dynamics of natural phenomena which may be approximated by models defined by discrete mappings. As traditional, we write these models generically as $x_{t+1} = f(x_t, a)$, where f is a nonlinear function, x_t is a real variable representing some quantity of interest as measured at time t and a is a real parameter. For simplicity, we start considering one variable and one parameter. For any particular generation t, the state and stability of possible solutions of the model are determined from the function $f_t(x, a)$ obtained by composing f with itself t times. Discrete models are frequently investigated by studying the behavior of

[1] E-mail: jason@hlrserv.hlrz.kfa-juelich.de

SSDI 0378-4371(94)00072-2

sequences of *numbers* generated with finite precision by iteration, starting from some initial condition. For example, the characterization of dynamical behaviors involves frequently the numerical determination of the so-called stable and unstable manifolds by, respectively, forward and backward iterating equations of motion from specific sets of initial conditions. In this paper, rather than studying sequences of numbers generated with finite precision, we wish to concentrate on the analytic properties of the infinite hierarchy of functions $\{f_t\}$ which underlie all iterative processes. As we hope to make clear in what follows, sequences of numbers are relatively simple consequences of the properties of this hierarchy of functions and, in particular, of a very special system-dependent *invariant entire limiting function* to which the dynamics must necessarily converge.

To fix ideas we elect the *quadratic* map

$$x_{t+1} = f(x_t, a) = a - x_t^2, \qquad t = 0, 1, 2, \ldots \tag{1.1}$$

as the main model to help implementing a systematic method to study limiting functions generated by iterating equations of motion. The state and stability of a system $f(a, x_t)$ for a given set of parameters and given t is defined by equations which may be formally represented as power series. For Eq. (1.1) the power series after t iterates is

$$f_t(x, a) = p_k(a)x^{2^t} + \cdots + p_1(a)x^2 + p_0(a), \tag{1.2}$$

where the coefficients $\{p_k(a)\}$ are different for every generation t. Since there are no singularities in any of the $f_t(x, a)$ and also no upper bound for the number of iterates, the generic limit for $t \to \infty$ of this hierarchy of functions for an arbitrary $f(x_t, a)$ is clearly an entire function, not a polynomial. From Eq. (1.2) we see that the asymptotic *limiting function* $\lambda(a, x)$ obtained after an infinite number of iterates is of the form

$$\lambda(x, a) = \sum_{j=0}^{\infty} P_j(a)x^{2j}. \tag{1.3}$$

The iterative process implied by Eq. (1.1) and similar ones certainly fixes the functional interdependence of every $P_j(a)$ on the parameter a. Now, instead of choosing to start with a one-parameter function we could also have taken a mapping more general in that while still maintaining a x^{2j} dependence on the variable, would be allowed to contain *many more* parameters. One fruitful example involving just two parameters is [1]

$$x_{t+1} = f(x_t, a, b) = (x_t^2 - a)^2 - b, \tag{1.4}$$

which is simply the second iterate of the quadratic map with a of the second iterate replaced by an arbitrary b. For Eq. (1.4), the relation between the several limiting coefficients P_j (depending now on two parameters) is much more complicated. But the existence of more control parameters allows simultaneously much more freedom and richness in dynamical behavior. Let us assume for a moment that the several P_j which appear in a given power series $\lambda(x, a,)$ like Eq. (1.3) could be generated from some not yet determined z-map (for "zero" map or, perhaps more appropriately at this stage,

for "Zauber" map) in a way such as to reduce the limiting entire function to one of the familiar elementary functions of mathematical physics. Three such limiting cases resembling the infinite series generated by the quadratic map could be, for example,

$$\cosh(x) = 1 + \frac{x^2}{2!} + \frac{x^4}{4!} + \frac{x^6}{6!} + \cdots, \tag{1.5a}$$

$$\cos(x) = 1 - \frac{x^2}{2!} + \frac{x^4}{4!} - \frac{x^6}{6!} + \cdots, \tag{1.5b}$$

$$\frac{\sin(x)}{x} = 1 - \frac{x^2}{3!} + \frac{x^4}{5!} - \frac{x^6}{7!} + \cdots. \tag{1.5c}$$

The infinite series corresponding to a Tchebicheff polynomial or to elliptic functions are more sophisticated examples. From the expressions above one recognizes that by appropriate choice of coefficients the same formal expansion in powers of x^2 may produce several different final "dynamics", characterized here by the properties of the well-known functions on the left-hand side of the equations. An interesting question seems then to be under which conditions it is possible to write simultaneously *all* coefficients recursively as functions of a very small number of parameters. Then, after this is done, to investigate for which values of these parameters one finds "resonances" between all coefficients of the infinite series such as to produce properties of interest. If such resonances might indeed be obtained by iterating some underlying z-map, the difficulty in determining the map would be mainly due to the fact that one does not know on how many parameters it might depend and which specific values of them should be used to produce particular limits such as those exemplified by Eqs. (1.5a–c). How can we find z-maps? How to solve the *Umkehrproblem* i.e. the problem of reversing an infinite power series into a z-map? Is it possible to "back-telescope" an infinite series into an elementary nonlinear *seed* which when iterated reproduces the whole power series? We have observed that all these questions are very much related to group properties of the set of zeros of the aforementioned invariant entire function and of the functions leading to it. Thus, it seems important to investigate the dynamical properties of the infinite number of zeros of these functions as they arise, generation after generation, in iterates of familiar maps.

The purpose of this paper is to discuss (in the next section) a systematic method for monitoring simultaneously the movement of all zeros of any arbitrary function, and to apply it to situations of particular interest in the study of dynamical systems. As shown by the examples below, the method is easy to apply and very helpful. This paper may be also considered as an attempt towards understanding (i) whether sequences of algebraic or transcendental functions generated by iterating z-maps may eventually lead to limiting entire functions which, in spite of being different, would share classes of identical properties under transformations, and (ii) whether limiting functions might be reduced to familiar infinite series (representing elementary functions such as those in Eq. (1.5), for example) or even to finite series, i.e. to polynomials. To this end we will consider here the dynamical evolution of the set of all generations of zeros on the complex plane for families of algebraic functions generated by some well studied maps.

2. The simultaneous interplay of all zeros

The choice of using real variables and parameters in Eq. (1.1) is primarily intended to reflect the *real* character of an actual measurement of an interesting quantity for some natural phenomena. There is, however, no intrinsic need for the dynamics to be restricted *a priori* over the reals. A more natural choice seems to be one similar to that done when dealing with, for example, electromagnetism, fluid dynamics or quantum mechanics: to base the analysis directly on a formulation constructed over the complex field along with a prescription on how to extract and interpret real and imaginary quantities associated with it. This is the key idea that will be explored in the paper. The remainder of this section is dedicated to the problem of calculating all zeros for arbitrary equations of motion. We start by first considering the calculation of zeros corresponding to period-1 dynamics (fixed points) for the quadratic map.

For the quadratic map the two possible period-1 zeros might be easily obtained by solving the quadratic equation $x^2 + x - a = 0$ for x:

$$x_s = (-1 + \sqrt{1+4a})/2 \qquad \text{and} \qquad x_u = (-1 - \sqrt{1+4a})/2. \tag{2.1}$$

These zeros might be either real or complex, depending on a. They were easy to obtain because according to Neugebauer [2], at least from around 1700 B.C. one knows how to solve a quadratic equation. But as nonlinear equations similar to Eq. (2.1) are iterated more and more, we run out extremely quickly of closed formulas for determining analytically (i) the possible physical orbits (subsets of the real zeros) (ii) whether these orbits are stable or not, and (iii) the extension of their respective domains of stability. Not knowing how to proceed analytically, we devise and implement a numerical strategy to obtain such important informations. As will become clear from what follows, knowledge of the simultaneous interplay of all zeros of the hierarchy of functions produced by iterating the equations of motion is essential for understanding the dynamics. By "simultaneous interplay" we mean the simultaneous displacements of all zeros in the complex plane as parameters are varied. As parameters are changed, zeros which were initially separated in the complex plane may collide, thereby producing detectable physical phenomena. Familiar *bifurcation* phenomena involve the transmutation of a pair of complex conjugate zeros into a pair of real ones (which remain conjugated quantities in a properly *extended* field). Bifurcations must occur by definition along the real line. We want to be able to investigate questions such as, e.g. is it possible to have collisions between different pairs of complex zeros happening "deeply" in the complex plane, i.e. not on the real axis? Under which conditions do they occur? Are collisions happening on the real line accompanied by other collisions happening deeply in the complex plane? Are parameter values at which zeros collide determined from the outset by the algebraic closure imposed by the equations of motion? Or more precisely, by the field of numbers defined by the parameters and initial conditions associated with the equations of motion? If independent deep collisions are possible, what type of phenomena do they produce along the physical horizon defined by the real axis? Is it possible to recognize and detect such events from measurements done exclusively along this horizon? Notice

that although in this paper we will concentrate on the dynamics of polynomial mappings with real coefficients, the approach used can be trivially adapted to deal with generic situations in which coefficients are complex numbers and the models are defined by arbitrary functions, transcendental or not.

Suppose that for a fixed value of a one needs to find all possible values of x that satisfy a generic algebraic or transcendental equation

$$f(x,a) = 0, \tag{2.2}$$

though of as representing an equation of motion in what follows. We find that a convenient way of studying all zeros is to consider all equations of motion as embedded in the "generalized" space where the most unconstrained possible dynamics lives. "Most unconstrained" means having all variables and parameters considered from the beginning over the complex field, on an equal footing. For Eq. (2.2) (which to simplify the discussion is assumed to depend only on a single variable and on a single parameter) the generalized space is four-dimensional, characterized by coordinates $(x,a;\xi,\alpha)$ obtained by *complexifying* the dynamics via the replacements $x \to x + i\xi$ and $a \to a + i\alpha$ in the equation of motion. Here α and ξ are real quantities and $i \equiv \sqrt{-1}$. The pair (x,a) correspond to the usual real variable and parameter, respectively, while the pair (ξ,α) are their "virtual" duals. The complexification has the effect of conformally splitting the original equation of motion into two useful functions: its real and imaginary parts, namely,

$$f(x + i\xi, a + i\alpha) = U(x,a;\xi,\alpha) + iV(x,a;\xi,\alpha), \tag{2.3}$$

in which, by construction, U and V are always real functions of real quantities. If only the projection for real parameters is of interest, one sets simply $\alpha = 0$ and considers the dynamics on the particular three-dimensional slice defined by

$$f(x + i\xi, a) = U(x,a;\xi) + iV(x,a;\xi). \tag{2.4}$$

The functions U and V are useful because they allow employing simple two-dimensional diagrams, "snapshots", to study the dynamics of the zeros. In the $U \times V$ framework, the original problem of finding all zeros of Eq. (2.2) for a given value of the parameter a translates into calculating all pairs (x,ξ) which satisfy simultaneously the fundamental equations

$$U = 0 \qquad \text{and} \qquad V = 0. \tag{2.5}$$

By comparing Eqs. (2.2) and (2.4) one sees that ξ acts physically like a *ghost* or *hidden* variable and that the rule of the game over the real field is to make virtual contributions V invisible, i.e. to vanish identically permanently. Since the ghost variable ξ appears in both U and V, we may say that the dynamics measured over the real universe U will necessarily display echoes from the virtual reality defined by V, and vice-versa.

Since U and V are constructed to be always real functions, the zeros that we are looking for may be obtained by discretizing a region of interest and plotting the *parity*

of U and V in that region. We say that the parity of U is *positive* on a point of the generalized space if $U > 0$ at that point, and *negative* if $U < 0$. Similarly for V. The problem of plotting the parity of U and V simultaneously on a single two-dimensional diagram is then equivalent to a "four-color" problem, i.e. equivalent to painting the region of interest with four colors representing the relative magnitudes of U and V in every point of the region. In the figures below we paint each point, "pixel", with a color or shading as follows:

$$\begin{aligned}
&\text{white} \quad \text{if} \quad (U>0, V>0) \equiv (+,+),\\
&\text{black} \quad \text{if} \quad (U>0, V<0) \equiv (+,-),\\
&\text{purple} \quad \text{if} \quad (U<0, V>0) \equiv (-,+),\\
&\text{yellow} \quad \text{if} \quad (U<0, V<0) \equiv (-,-).
\end{aligned}$$

The names "purple" and "yellow" denote colors convenient in that when printed as gray-scales with non-color printers, produce high contrast half-tones intermediate between black and white. In the figures below, purple produces the shading closer to black while yellow produces the shading closer to white. For completeness one should also define parities and shadings for those points at which U and/or V vanish identically. There are however good reasons to make such definitions not really necessary for our purposes here: first, it is in general hard to hit zeros *precisely* using a numerically discretized covering of a continuous domain; second, even if we hit them, such isolated pixels are virtually invisible on the figures under the relatively high resolution of 300 dots-per-inch used here to produce them as color PostScript bitmaps. Apart from minimizing waist of computer time, as one may easily convince oneself by looking at the figures below, four colors are perfectly enough to characterize and follow the dynamics precisely and unambiguously whenever the graphical resolution is sufficiently high. The zeros of $U = 0$ correspond to some of the border *lines* between regions with *two* different colors. Similarly for V. Simultaneous zeros of $U = 0$ and $V = 0$ correspond clearly to those very particular *points* where regions with *four* different colors meet.

The $t = 1$ horizontal row in Fig. 1 shows an application of the ideas above to investigate the dynamics of the fixed points x_s and x_u, Eq. (2.1), of the quadratic map as the parameter a is varied. In this case

$$U(x,a;\xi) = x^2 - \xi^2 + x - a, \qquad V(x,a;\xi) = (1+2x)\xi. \tag{2.6}$$

Notice the freedom along the line $x = -1/2$. Individual figures show all zeros of the equations obtained after t iterates, as indicated. Each set of four horizontal figures shows the zeros for a constant t and for $a = -1$, $-1/4$, 0 and $3/4$, chosen because the real fixed point denoted by x_s is known to be stable only for $-1/4 \leq a \leq 3/4$. For $a = -1$ and $t = 1$ there are two complex conjugate zeros, the intersections of the two parabolas with the vertical line $x = -1/2$. For $a = -1/4$ these zeros become real numbers by colliding with the physical horizon represented by the axis $\xi = 0$. This event corresponds to the characteristic saddle-node bifurcation leading to stable period-1 dynamics. Beyond

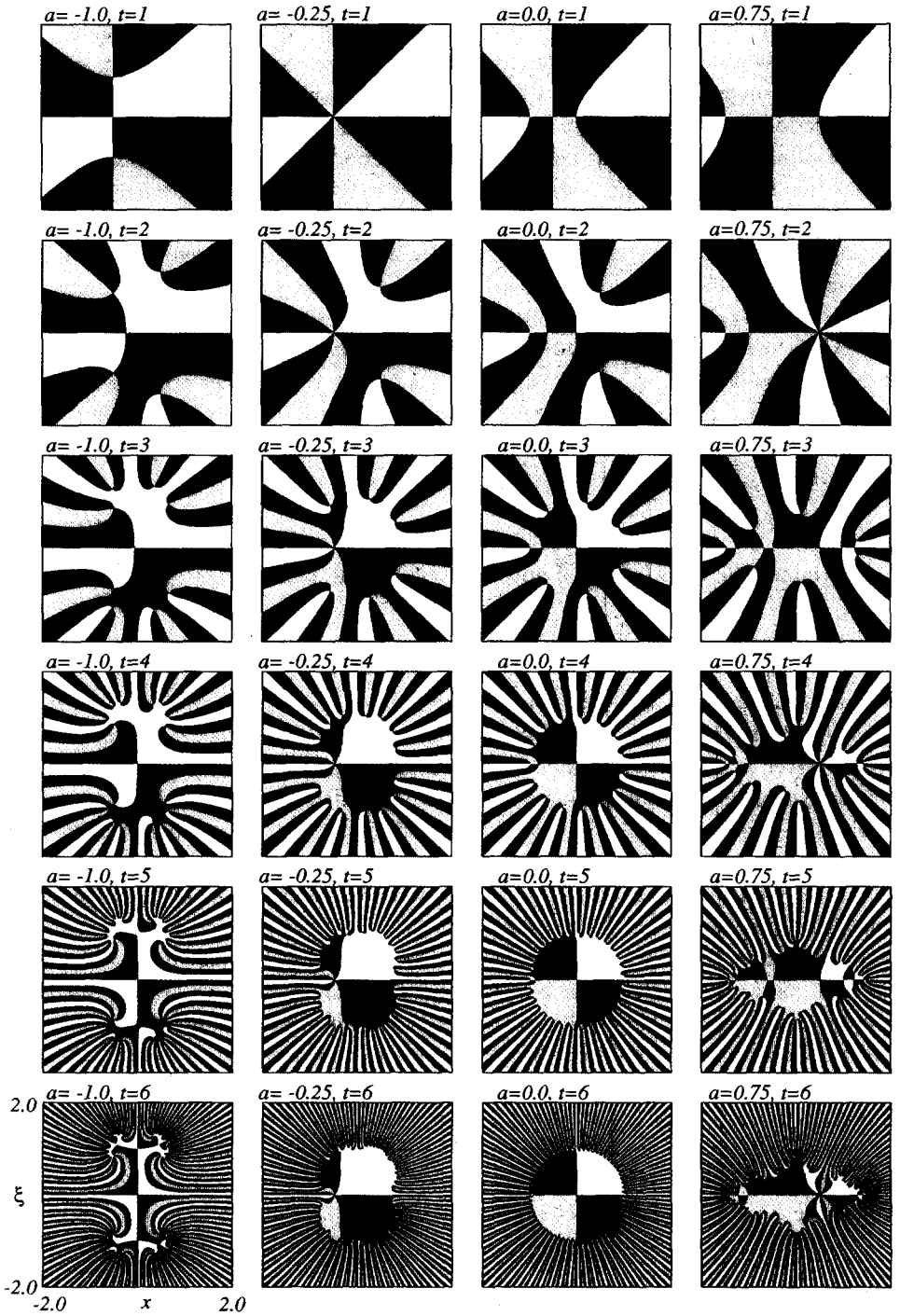

Fig. 1. Evolution of all zeros for the first six iterates of the quadratic map, Eq. (1.1). Zeros are the points where domains of four different colors meet. The meaning of the colors is explained in Section 2. The scales and variables shown for $a = -1, t = 6$ are the same for all other values of a and/or t in the figure. Each square in this and similar pictures further on contains 450×450 pixels.

$a = -1/4$ the stable fixed point x_s moves towards the right while the unstable one, x_u, moves towards the left, always along the $\xi = 0$ axis. Now, we ask: what happens in this same interval of parameters to all other zeros which correspond to motions of higher periodicities (and which are all unstable in this interval)? In other words, were are the zeros of the equations corresponding to period-2, period-3, etc. located in the $x \times \xi$ plane for the interval of parameters where period-1 is stable? The situation for the generations $t = 2, 3, 4, 5$ and 6 may be seen along the other horizontal rows of Fig. 1, as indicated. The detailed dynamics of these generations will be discussed below. We start by discussing in the next section the behavior as seen along the $a = 0$ vertical column. For $a = 0$ the fixed point at finite distance with the largest basin of attraction along the real axis is the superstable fixed-point $x = 0$ which, therefore, is the most likely finite attractor to be detected experimentally. Note that $x = -1$ is another possible real orbit having, however, a measure-zero basin of attraction along the real axis consisting of just two isolated points: $x = -1$ and $x = 1$. But the real axis is the "wrong" direction of attraction for $x = -1$.

3. The quadratic map for $a = 0$ and the Kreisteilung problem

The purpose of this section is to show that for the particular value $a = 0$ of the quadratic map it is possible to identify *analytically* on the basin boundary the presence of roots of unity which also appear in the very famous *Kreisteilung* problem studied by Gauss (1777-1855), namely the problem of factoring $x^p - 1$ in order to find conditions on the power p such that a regular $p-$gon could be constructed using only the tools allowed by Euclid, i.e. ruler and compass. The very interesting and long history of the problem of dividing a circle into equal parts and its associated *cyclotomic equation* is told in an extremely beautiful and actual little book written one hundred years ago by Klein [3]. We believe the identification of these two problems to be of importance because the experience already accumulated while studying cyclotomic equations provides very useful ideas on how to attack related problems for different parameter values and for much more complicated equations of motion. Of immense interest is the possibility of using exact representations of roots of -1 of all orders to investigate with *absolute numerical precision* the dynamics happening on invariant manifolds of the fixed point $(x = -1, \xi = 0)$.

Thanks to de Moivre's theorem, the zeros of the cyclotomic polynomials $x^p - 1$ are known to be points equally spaced on the circumference of the unit circle on the complex plane, the vertices of a regular polygon of p sides. This fact allows one to decompose $x^p - 1$ into linear factors over the complex numbers as follows:

$$x^p - 1 = \prod_{k=0}^{p-1} \left(x - \{ \cos \frac{2\pi k}{p} + i \sin \frac{2\pi k}{p} \} \right) = \prod_{k=0}^{p-1} \left(x - e^{2\pi i k/p} \right). \tag{3.1}$$

But rather than this quite general mathematical factorization over the complex field one

may also use its linear factors to investigate which suitable combinations of them will produce a physical factorization of the stable dynamics over the reals, over rationals and in particular and much more interestingly, over some specific rings and finite fields on particular algebraic extensions. As mentioned before, the bifurcation diagram corresponding to the quadratic map has a stable fixed point (period-1 orbit) for all parameter values in the interval $-1/4 \leq a \leq 3/4$. For $a = 0$ one has the so-called [4] "superattractive" or "superstable" orbit. (For a recent discussion of the bifurcation diagram for the quadratic map see, for example, Section 3 and Fig. 1 of Ref. 1a.) The $t-$th generation of functions underlying superstable $a = 0$ orbits for the quadratic map is given by

$$x_{t+1} = -x_t^2 = -x_0^{2^t}. \tag{3.2}$$

The associated limiting functions $\Lambda(0,x)$ and $\lambda(0,x)$ are in this case

$$\Lambda(x,0) \equiv x + \lambda(x,0) = x + \lim_{t\to\infty} x^{2^t}. \tag{3.3}$$

The properties of these functions may be studied by considering the limit of the properties of subsequent *generations* of functions defined by

$$\Lambda_p(x,0) = x + x^{p+1} = x(x^p + 1), \tag{3.4}$$

where $p = 2^t - 1$. Eq. (3.4) shows clearly that cyclotomic equations appear as fundamental components of the invariant limiting function defining the basin boundary or, in other words, of the stable manifold of the fixed point $x = -1$ (and $\xi = 0$). Note the important fact that not every possible cyclotomic equation appears as a factor of the infinite family of functions generated by the quadratic map. But the zeros of every possible cyclotomic equation live on the closure of those zeros of the functions that appear as factors, generated by the dynamics of the map. All together, they form the basin boundary, or equivalently, the $F-$set.

The $a = 0$ column in Fig. 1 shows the location on the $x \times \xi$ plane of a few families of zeros for Eq. (3.4), with the conspicuous presence for every t of the zero at the origin. The dynamics of the quadratic map for any real value of a is particularly instructive when considered in the $x \times \xi$ plane. When $a = 0$ one has the following two-dimensional map

$$(x,\xi) \mapsto (\xi^2 - x^2, -2x\xi). \tag{3.5}$$

For conditions located *inside* the unit circle, iterates of Eq. (3.5) always converge asymptotically to the superattracting fixed point at the origin. Initial conditions *outside* the circle lead always to convergence towards the fixed point located at infinity. For initial conditions precisely *on the circle* there are two possible types of asymptotic behavior: periodic or aperiodic i.e. "chaotic", depending on the commensurability of the initial condition and the infinity of numbers of the form

$$\cos\frac{2\pi k}{p} + i\sin\frac{2\pi k}{p}, \tag{3.6}$$

for all possible integers k and $p = 2^t - 1$. The fixed point $(x, \xi) = (-1, 0)$ belongs to the very particular frontier set defined by those points lying exactly on the unit circle and which separate the domains of attraction of the two stable points: $(0, 0)$ and infinity. The fixed point $(-1, 0)$ is a very stable attractor for dynamics happening on the unit circle. *There is absolutely no mechanism allowing iterates to move out of the circle if one starts the iteration from a point located exactly on the unit circle and performs all computations with absolute precision.* The equation of the circle guarantees this. Therefore, all dynamics occurring within the boundary is perfectly stable as long as one moves exactly "parallel" to the border. Any slight perturbation "perpendicular" to it will be quickly amplified by the nonlinearity in the equations of motion, forcing the orbit to diverge away from the border. From this example one sees that *if it were always possible to perform computations with absolute precision, then there would be no "unstable" dynamics.* The basic difference between fixed points is simply that while some points are able to attract quite "isotropically" in the space of variables (i.e. along a dense set of different directions), others can attract only along very specific directions. This observation makes it natural to classify fixed points and periodic orbits according to the dimension of their attracting set.

While it is possible to recognize the aforementioned facts analytically from Eq. (3.5), any attempt of following numerically an exact orbit using only finite-precision arithmetics on a computer, "shadowing", is bounded to fail due to the accumulation of round-off errors, with the dynamics escaping the frontier and "converging" after a relatively small number of iterates to one of the isotropically attracting fixed points, zero or infinity in the present example. Numerical computations using polar coordinates prevent iterates from escaping the unit circle. But then finite-precision arithmetics has the (deleterious) effect of continuously forcing the system to jump between different allowed orbits living on the circle. Thus, finite-precision arithmetics is the sole responsible for the "butterfly effect" of Lorenz: finite-precision arithmetics will always necessarily induce intolerable perturbations in the dynamics. The severe limitations imposed by finite-precision arithmetics are more easily seen when trying to make "long walks" along $F-$sets (i.e. basin boundaries). All behaviors described above for $a = 0$ continue to exist when $a \neq 0$, the difference being that the frontier set is much more complicated to characterize and probe analytically. Further, there seems to be no reason to expect different behavior when the number of variables and/or parameters is larger than one. If it were always possible to perform computations with absolute precision, the question of ascertaining the final attractor would be reduced to a problem of determining in which Riemann sheet initial conditions are located, and to which particular field of numbers they belong. The passage from any given initial condition to a final attractor presents no intrinsic difficulty and is always uniquely defined by the powerful algebraic closure imposed by the equations of motion. From a theoretical point of view, the impossibility of ascertaining final attractors, i.e. of predicting the future, seems to originate exclusively from difficulties in (i) determining accurately the field of numbers to which initial conditions and parameters belong and, (ii) performing all needed arithmetics with absolute precision. In nature, after a trajectory is started from some initial condition, arbitrarily

small perturbations of parameters (noise) might induce transitions from the original trajectory to another possible one which may have quite different asymptotic properties. While it is certainly possible to approximate any irrational number by rational ones, in absence of perturbations, a trajectory started from an arbitrary irrational initial condition will remain forever bounded to similar irrationals, as imposed by the algebraic closure implicitly defined by the equations of motion.

4. What are generic basin boundaries between domains of convergence made of?

In 1906, Fatou [5] addressed the problem of delimiting the frontiers between domains of convergence for iterated functions $f(z)$ in the complex plane. He concluded stating that *"L'etude de certains cas particuliers montre qu'effectivement les frontières sont en général de nature compliquée"*. In 1917 he published two further notes [6,7] discussing once again the *Frontière F*. Then, it was possible for him to profit from the important concept of *normal families*, introduced by Montel [8]. Fatou remarked [7] then that the frontier F had the property that *"En un point p de F les fonctions f_t ne peuvent pas former une suite normale, au sens de Montel"*, which translates into one of the definitions in use today[9-16]:

Definition 1. The F-set consists of those points at which the sequence $\{f_t(z)\}$ is not normal, in the sense of Montel.

In the same note [7] Fatou observed that " *...F est le dérivé de l'ensemble des antécedents d'un quelconque de ses points.*" Subsequently, he further discussed this subject in three long *Mémoires* [17]. Concerning the derived set, Julia wrote in his *Mémoire* of 1918, Ref. [18], page 48: *"La question qui domine cette étude est la suivante: un point z étant donné dont les conséquents $z_1, z_2, \ldots, z_n, \ldots$ forment un ensemble e, quelle sont les proprietés de l'ensemble e', derivée de l'ensemble e."* The derived set is the set of all accumulation points. The set which contains a given set along with all accumulation points of the given set defines the *closure* of the given set. Thus, the essence of the above quotations appears in another definition of the F-set:

Definition 2. The F-set is the closure of the set of repelling periodic points.

These two definitions discussed by Fatou[5-7,17] and by Julia [18] are the definitions commonly used today to characterize the frontier between different domains of convergence of iterated functions ("power series"), as may be seen, e.g., from Refs. [9-16] and from the works quoted therein.

In the $\alpha = 0$ slice of the generalized space the dynamics of Eq. (1.1) is defined by the system of equations

$$x_{t+1} = a - x_t^2 + \xi_t^2, \tag{4.1a}$$

$$\xi_{t+1} = -2x_t\xi_t, \tag{4.1b}$$

where ξ_t is the ghost variable associated with x_t. Fig. 1 shows several additional $x \times \xi$ slices of the generalized space for $a = -1.0, -1/4, 0.0$ and $3/4$ and for $t = 2, 3, 4, 5$ and 6. From the evolution of the zeros seen in the columns $a = -0.25$ and $a = 0.75$ of Fig. 1 it is easy to recognize which geometrical figure the union of the zeros of iterated maps build in the generalized space: they build exactly the F-set. From this observation and from the discussion in the previous section we find convenient the following alternative statement:

Definition 3. The F-set is formed by the closure of all zeros of the infinite sequence of functions $\{f_t(z)\}$, including Λ, except for those zeros which belong to stable orbits.

This alternative definition tells in simpler terms which mathematical objects compose generic frontiers between domains of convergence of arbitrary power series. One practical advantage is that it is not a purely existence statement from which one might not construct the whole set, in principle. Starting from $t = 1$ this last formulation provides a clear prescription about how to systematically construct F-sets precisely. Rather than the closure, in practical applications a moderately large set of zeros together with some of their preimages provides frequently excellent approximations of the $F-$set. An idea of how good this works may be obtained from Fig. 1. In Section 7 below we argue that, in essence, analogous zeros are the mathematical objects which underly the so-called invariant manifolds of higher-dimensional dynamical systems, responsible for defining the boundaries of domains of stability in phase-space of generic physical models.

5. The genesis of periodic dynamics in the frontiers

We now describe how periodic motions arise in the frontiers between different domains of convergence for some power series generated by infinite sequences of quadratic compositions. These compositions are of importance because quadratic terms are the most elementary forms of nonlinearities appearing in series expansions of arbitrary equations of motion. Thus, results for quadratic compositions can be expected to be of relevance for many different practical applications. We present a few results for the quadratic map here.

5.1. *Results for* $a = 0$

In addition to the attractor located at $-\infty$, for $a = 0$ the quadratic map has two other real fixed points: the stable superattracting point $x = 0$ and the unstable point $x = -1$. Using $f_t(x, a)$ to represent the t-th composition of $f(x, a)$ with itself, these two points are obtained by solving the equation

$$p_1(x, 0) \equiv x - f_1(x, 0) = x + x^2 = x(1 + x) = 0, \tag{5.1}$$

where $f_1(x, 0) \equiv f(x, 0)$. Along the real axis, the only way to reach the attractor $x = -1$ is by starting iterations exactly from either $x = -1$ or $x = 1$. The attractor

$x = -1$ is totally inaccessible from other initial conditions along the real axis. For initial conditions in the open interval $-1 < x < 1$ the iterative process generates orbits (i.e. sequences of numbers) which are simply pre-periodic transients leading to the fixed point $x = 0$. The open intervals $-\infty < x < -1$ and $1 < x < \infty$ contain all real initial conditions producing pre-periodic orbits leading to the fixed point $x = -\infty$. The characteristic feature here is that initial conditions corresponding to pre-periodic transients leading to the fixed points $-\infty$ and 0 appear as open and dense sets, while those of $x = -1$ are not, being isolated points along the real axis.

An infinite family of functions is generated by iterating $x_{t+1} = -x_t^2$ further and further. Ideally, one would like to consider the properties of the limiting function obtained after infinite iterates. Since in general this liming function is not expected to reduce to a known function of the mathematical physics, we proceed by investigating the limit of the regularities that appear consistently at every new iterate, hoping in this way to understand the global picture in the limit of infinite iterates. Four additional polynomials of the infinite sequence are

$$p_2(x,0) = x + x^4 = x(1+x)(1-x+x^2), \tag{5.2a}$$

$$p_3(x,0) = x + x^8 = x(1+x)(1-x+x^2-x^3+x^4-x^5+x^6), \tag{5.2b}$$

$$p_4(x,0) = x + x^{16} = x(1+x)(1-x+x^2)(1-x+x^2-x^3+x^4) \times (1+x-x^3-x^4-x^5+x^7+x^8), \tag{5.2c}$$

$$p_5(x,0) = x + x^{32} = x(1+x)(1-x+x^2-x^3+\ldots-x^{29}+x^{30}). \tag{5.2d}$$

Apart from the zeros $x = -1$ and $x = 0$ corresponding to the aforementioned real fixed points, these expressions contains many other zeros, defined by the additional polynomial factors. A relevant question is then to investigate the dynamics observed when using such zeros as initial conditions. Since we expect most of these zeros to be complex numbers, it is necessary to consider the dynamics in the $x \times \xi$ plane of the generalized space. We start studying the dynamics of the zeros of $p_2(x,0)$.

The two not yet determined zeros of $p_2(x,0)$ are

$$1 - x + x^2 = (x - \frac{1+\sqrt{-3}}{2})(x - \frac{1-\sqrt{-3}}{2}) = 0. \tag{5.3}$$

Although trivial to obtain, the above representation in terms of square roots is not the best suited for our present purposes. A more convenient representation is obtained by observing that the zeros of Eq. (5.3) may be also represented using cubic roots as follows

$$1 - x + x^2 = (x - s^{1/3})(x - s^{5/3}) = 1 - [s^{1/3} + s^{5/3}]x + s^{1/3}s^{5/3}x^2 = 0, \tag{5.4}$$

where $s \equiv -1$. For later use we observe that $s_3 \equiv s^{2/3} + s^{4/3} = -[s^{1/3} + s^{5/3}] = -1$. From Eq. (5.4) one recognizes that the four zeros of $p_2(x,0)$ are in fact

$$z_1 = s^{0/3} = 0, \quad z_2 = s^{1/3}, \quad z_3 = s^{3/3} = -1, \quad z_4 = s^{5/3}, \tag{5.5}$$

and that their dynamics under the map is as follows:

$$f(z_1,0)=z_1, \quad f(z_2,0)=z_4, \quad f(z_3,0)=z_3, \quad f(z_4,0)=z_2. \tag{5.6}$$

Therefore, in addition to the real fixed points already obtained from $p_1(x,0)$, p_2 defines a (complex) period-2 orbit $z_2 \rightleftharpoons z_4$ which lives in the frontier set in the generalized space.

Repeating the analysis for $p_3(x,0)$ one finds the following periodic cycles living in the frontier:

$$\text{period-3:} \quad s^{1/7} \to s^{9/7} \to s^{11/7} \to s^{1/7}, \tag{5.7a}$$

$$\text{period-3:} \quad s^{3/7} \to s^{13/7} \to s^{5/7} \to s^{3/7}, \tag{5.7b}$$

in addition to the real fixed points $s^{0/7}$ and $s^{7/7}$. These cycles produce the following factors through a well-defined combinatoric rule:

$$\phi_1 = (x-s^{1/7})(x-s^{9/7})(x-s^{11/7}) \tag{5.8a}$$

$$= (x+s^{2/7})(x+s^{4/7})(x+s^{8/7}) \tag{5.8b}$$

$$= 1+[s^{6/7}+s^{10/7}+s^{12/7}]x+[s^{2/7}+s^{4/7}+s^{8/7}]x^2+x^3, \tag{5.8c}$$

$$\phi_2 = (x-s^{3/7})(x-s^{13/7})(x-s^{5/7}) \tag{5.9a}$$

$$= (x+s^{6/7})(x+s^{10/7})(x+s^{12/7}) \tag{5.9b}$$

$$= 1+[s^{2/7}+s^{4/7}+s^{8/7}]x+[s^{6/7}+s^{10/7}+s^{12/7}]x^2+x^3. \tag{5.9c}$$

Multiplying these two complex-conjugate polynomials one sees the essence of the mechanism which by very suitably combining roots of -1, produces factorization over real integers:

$$\phi_1\phi_2 = 1+s_7x+[3+2s_7]x^2+[2+3s_7]x^3 + [3+2s_7]x^4+[2+3s_7]x^5+x^6, \tag{5.10}$$

in which now the representation

$$s_7 \equiv (-1)^{2/7}+(-1)^{4/7}+(-1)^{6/7}+(-1)^{8/7} + (-1)^{10/7}+(-1)^{12/7} \equiv -1 \tag{5.11}$$

appears.

Analogously, among the zeros of $p_4(x,0)=0$ one finds the following cycles

$$\text{period-4:} \quad s^{1/15} \to s^{17/15} \to s^{19/15} \to s^{23/15} \to s^{1/15}, \tag{5.12a}$$

$$\text{period-4:} \quad s^{7/15} \to s^{29/15} \to s^{13/15} \to s^{11/15} \to s^{7/15}, \tag{5.12b}$$

$$\text{period-4:} \quad s^{9/5} \to s^{3/5} \to s^{1/5} \to s^{7/5} \to s^{9/5}, \tag{5.12c}$$

$$\text{period-2:} \quad s^{1/3} \to s^{5/3} \to s^{1/3}, \tag{5.12d}$$

in addition to the real fixed points $s^{0/15}$ and $s^{15/15}$. The points in the cycle of Eq. (5.12d) produce the factor already found in Eq. (5.4). The cycle in Eq. (5.12c) produces

$$1 - x + x^2 - x^3 + x^4 = [(x - s^{9/5})(x - s^{3/5})][(x - s^{1/5})(x - s^{7/5})], \quad (5.13a)$$

$$= [s^{2/5} + (s^{4/5} + s^{8/5})x + x^2][s^{8/5} + (s^{2/5} + s^{6/5})x + x^2], \quad (5.13b)$$

$$= 1 + s_5 x + (2 + s_5)x^2 + s_5 x^3 + x^4, \quad (5.13c)$$

where in Eq. (5.13c) the factorization over reals is obtained with the help of the representation

$$s_5 \equiv (-1)^{2/5} + (-1)^{4/5} + (-1)^{6/5} + (-1)^{8/5} \equiv -1. \quad (5.14)$$

The other two period-4 orbits in Eqs. (5.12a) and (5.12b) produce two fourth-degree polynomials over the complex field which when multiplied yield the real eighth-degree factor in Eq. (5.2c). This situation is totally analogous to what happened with the complex quadratic factors in Eq. (5.13b), which combine to give a real quartic factor, or already earlier, in deriving Eq. (5.10). The interesting point to notice here is that the whole iteration acts as a gear mechanism in which individuals gears, the different roots of -1, resonate to produce a factorization over the reals after the proper number of iterates. These resonances depend critically on families of very particular sums of certain complex numbers. In the present context, the sums are s_3, s_5, s_7, etc., as defined above, in which all individual terms are roots of unity. As it is easy to recognize from the expressions above, all polynomial factors over the reals are defined by non-trivial combinatorial problems involving such sums.

The two complex-conjugate factors producing the real eighth-degree polynomial in Eq. (5.2c) are

$$\Phi_1 = (x - s^{1/15})(x - s^{17/15})(x - s^{19/15})(x - s^{23/15}) \quad (5.15a)$$

$$= 1 + [s^{14/15} + s^{22/15} + s^{26/15} + s^{28/15}]x + [s^{2/5} + s^{2/3} + s^{4/5} + s^{6/5} + s^{4/3} + s^{8/5}]x^2 + [s^{2/15} + s^{4/15} + s^{8/15} + s^{16/15}]x^3 + x^4, \quad (5.15b)$$

$$\Phi_2 = (x - s^{7/15})(x - s^{29/15})(x - s^{13/15})(x - s^{11/15}) \quad (5.16a)$$

$$= 1 + [s^{14/15} + s^{22/15} + s^{26/15} + s^{28/15}]x + [s^{2/5} + s^{2/3} + s^{4/5} + s^{6/5} + s^{4/3} + s^{8/5}]x^2 + [s^{14/15} + s^{22/15} + s^{26/15} + s^{28/15}]x^3 + x^4. \quad (5.16b)$$

Multiplying them one obtains a factor over real integers:

$$\Phi_1\Phi_2 = 1 + w_{15}x + [4 + w_{15} + 3s_5 + 2s_3]x^2 + [5w_{15} + 4s_3 + 2s_5]x^3 + [8 + 7s_5 + 5s_3 + 3w_{15}]x^4 + [5w_{15} + 4s_3 + 2s_5]x^5 + [4 + 3s_5 + 2s_3 + w_{15}]x^6 + w_{15}x^7 + x^8, \quad (5.17)$$

where the new thing is the appearance of an alternative representation for the number 1, showing up again as a very particular sum of complex terms, namely,

$$w_{15} \equiv s^{2/15} + s^{4/15} + s^{8/15} + s^{14/15} + s^{16/15} + s^{22/15} + s^{26/15} + s^{28/15} = 1. \quad (5.18)$$

From the discussion above one recognizes the fundamental importance of algebraic integers in the dynamics and the very special role played by powers p/q of -1, for which p and q are not relative prime numbers. These results seem to show that dynamics may also be regarded as an application of Number Theory or else, that the "static" properties observed in Number Theory are in fact consequences of an underlying "hyper" dynamics, depending heavily on transformation properties between sets of algebraic extensions of numbers. At any rate, the above examples seem to leave little doubt about the existence of an extremely strong connection between dynamics and Number Theory.

5.2. *Results for* $a \neq 0$

After studying the behavior of the zeros in the frontier for $a = 0$, the next natural question is to ask whether the several regularities found survive changes of parameters. To illustrate typical behaviors happening when a parameter is changed, Fig. 2 shows the evolution of the zeros corresponding to the $t = 4$ generation of the quadratic map, together with the two fixed points (represented by squares and appearing here along the real axis; the open square is the unstable fixed point). The two zeros connected by a vertical line segment at $x = 0.5$ are those corresponding to the period-2 cycle which factors as shown by Eqs. (5.4) and (5.12d). They appear in every generation. For a increasing, after "colliding" with the real axis for $a = 0.75$ (left end of period-2 interval of stability), both period-2 zeros remain confined to the real axis: period-2 bifurcation. The three period-4 cycles of Eqs. (5.12a–c) are also represented on this figure. The cycles producing the factors Φ_1 and Φ_2 (Eqs. (5.15) and (5.16)) correspond to movements with well defined orientations around the frontier: Φ_1 produces a anti-clockwise circulation while Φ_2 produce a clockwise circulation. In contrast, Eq. (5.12c), containing the non-relative prime multiples of 15, produces a zig-zag pattern, indicated in the figure by the four points connected by the dashed line. For $a = 0$ the complex zeros contained in this cycle produce a factor over the reals.

From Fig. 2 one may recognize that all cycles determined for $a = 0$ continue to exist for $a < 0$ and for $a > 0$. This shows the importance of studying the cycles and factorizations composing the frontier for $a = 0$: although for arbitrary values of a it is not always possible to compute analytically the dynamics as for $a = 0$, systematic numerical work shows that the same periodic cycles living on the frontier for $a = 0$ continue to exist for rather large intervals of parameters. We conclude this section by observing that the above results are intended simply to illustrate possible applications of the methodology being proposed and the importance of considering all zeros simultaneously, not as an exhaustive discussion of the examples. A more detailed investigation of these and other examples will be presented elsewhere.

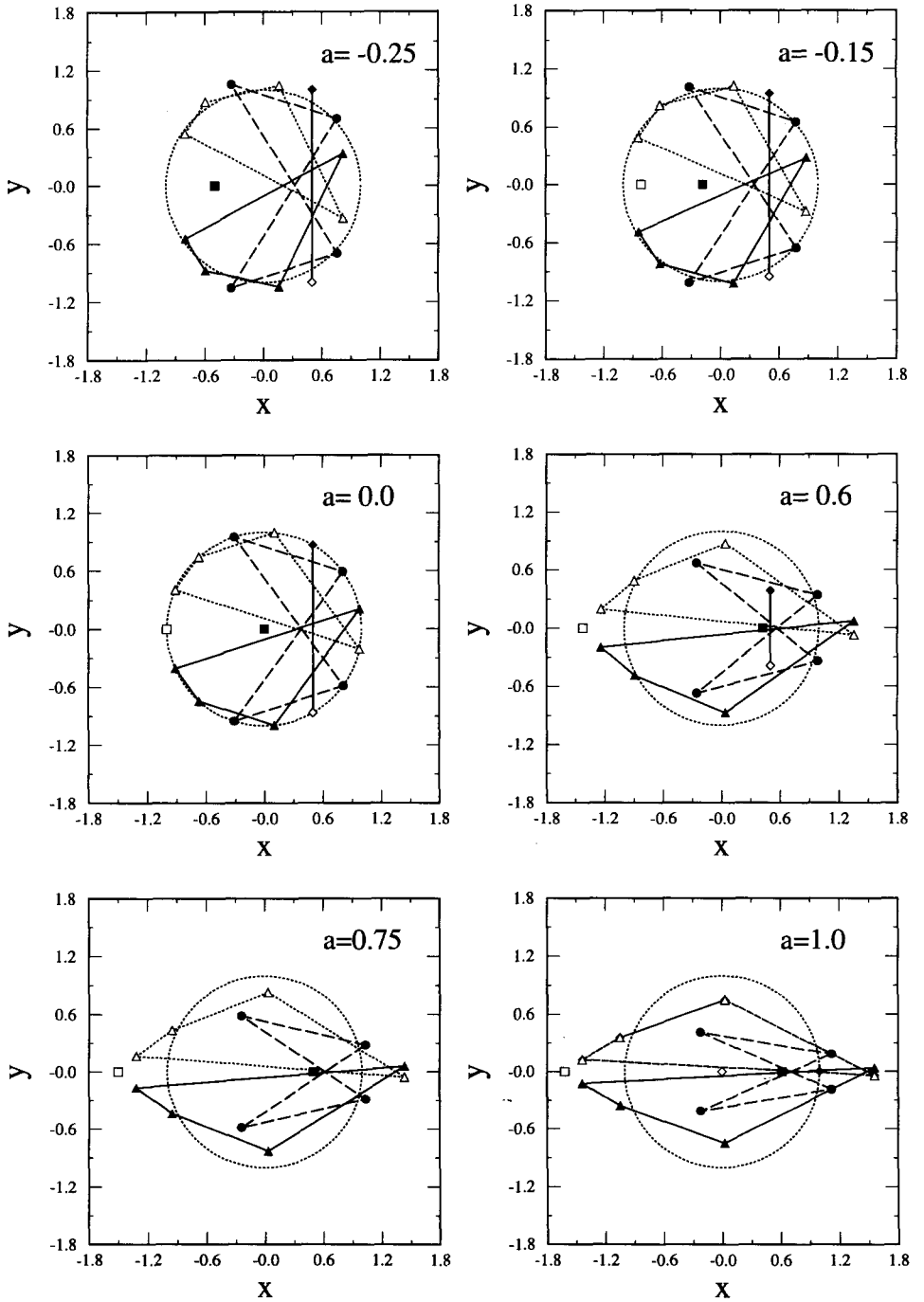

Fig. 2. Evolution of the cycles defined in Eqs. (5.12a–d), corresponding to the zeros of the fourth iterate of the quadratic map. The cycles survive parameter changes. The two real points not connected are the fixed points defined in Eq. (2.1). In this figure, $y \equiv \xi$.

6. The canonical quartic map: one variable and two parameters

We discuss now the evolution of the zeros for a more general model, Eq. (1.4), containing one variable and two parameters. This model was recently shown to be a sort of "canonical" model for studying dynamical behavior present in all systems with equations of motion reducible to series of quadratic compositions [1]. As shown in Fig. 3a, the parameter space of Eq. (1.4) contains many shrimp-like clusters of stability [1], the most prominent appearing centered along a cardioid defined parametrically by the equations

$$(a,b) = (p^4 - p, p^2) \qquad \text{and} \qquad (a,b) = (p^2, p^4 - p). \tag{6.1}$$

In the Appendix below it is shown that all parameter loci corresponding to superstable orbits of Eq. (1.4) are *self-inverse* curves, similarly to what happens with the branches forming the cardioid 6.1 displayed in Fig. 3b. From Fig. 3 one sees that the most easily discernible shrimps correspond to the period-1 shrimp centered at $(a,b) = (0,0)$ and the two period-3 shrimps located roughly at $(0.725561, 1.37824)$, along the upper branch $a = b^2 - \sqrt{b}$ of the cardioid, Eq. (6.1a), and $(1.37824, 0.725561)$, along the lower branch $b = a^2 - \sqrt{a}$. Exact values are given by $a = [(3 \pm \sqrt{5})/2]^{1/3}$, the real roots of $1 - 3a^3 + a^6 = 0$. We now consider the evolution of zeros on the $x_t \times \xi_t$ plane for parameters corresponding to the head of the period-1 shrimp, as shown in Fig. 4. The central column in this figure shows the zeros for the head while the other columns show the situation for two symmetrical displacements of $b = \pm 0.25$ along $a = 0$. Notice the rather different disposition of the zeros for $t = 1$. For $b \simeq 0$ the F-sets look like rounded squares, being both, however, homeomorphic to the circle obtained for $(a,b) = (0,0)$. While it is very difficult to anticipate the topology of F-sets, notice that the net effect of moving from $b = -0.25 \rightarrow b = 0.0 \rightarrow b = 0.25$ is close to a rotation of the domain of convergence. Fig. 5 shows the zeros as obtained along the diagonal $a = b$ around the *tail* $(a,b) = (1,1)$ of the period-1 cell. Along this diagonal the quartic map is simply the second iterate of the quadratic map and depends on a single parameter only. For $b = a$ the equation defining fixed points may be factored as

$$x - (a - x^2)^2 + a = (a + x - x^2)(1 - a + x + x^2) = 0. \tag{6.2}$$

For $a = 1$, this equation yields

$$\begin{aligned} x - (1 - x^2)^2 + 1 &= x(x+1)(1 + x - x^2) \\ &= x(x+1)\left(x - \frac{1+\sqrt{5}}{2}\right)\left(x - \frac{1-\sqrt{5}}{2}\right) = 0. \end{aligned} \tag{6.3}$$

The factor $1 + x - x^2$ defines the unstable fixed points that live on the F-set and that attract the dynamics on it. Notice that $(-1 + \sqrt{5})/2 \simeq 0.618\ldots$ is a famous irrational, the *golden mean*, telling how to divide a line segment into two pieces such that the ratio of the shorter piece to the larger equals the ratio of the larger to the whole segment. As discussed in Ref. 1a, at the tail of cells of stability one finds hysteretic behavior resulting

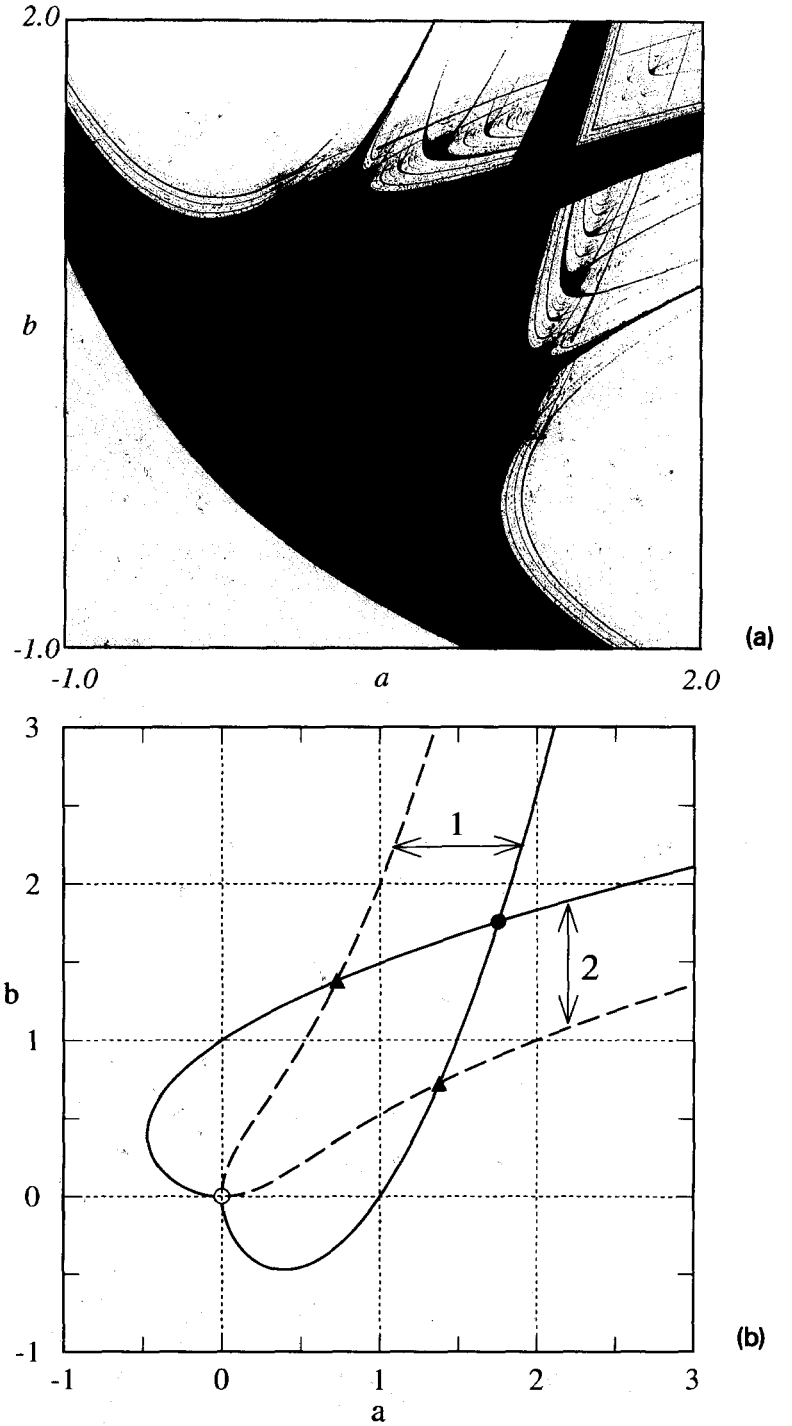

Fig. 3. (a) Multipliers for the canonical quartic $x \mapsto (a - x^2)^2 - b$, Eq. (1.4). In this figure, yellow indicates parameters leading to unbounded orbits, white represents chaos, i.e. absence of periodicity for bounded orbits, black(purple) indicates multipliers with negative(positive) parity. See Ref. 1a for definitions and details; (b) The cardioid where the most prominent shrimps live aligned. 1: $a = b^2 - b^{1/2}$, 2: $b = a^2 - a^{1/2}$. The open circle indicates the head of the period-1 shrimp while the three solid symbols indicate heads of period-3 shrimps. Two prominent non-diagonal 3-shrimps have their heads defined by the real zeros of $1 - 3a^3 + a^6 = 0$.

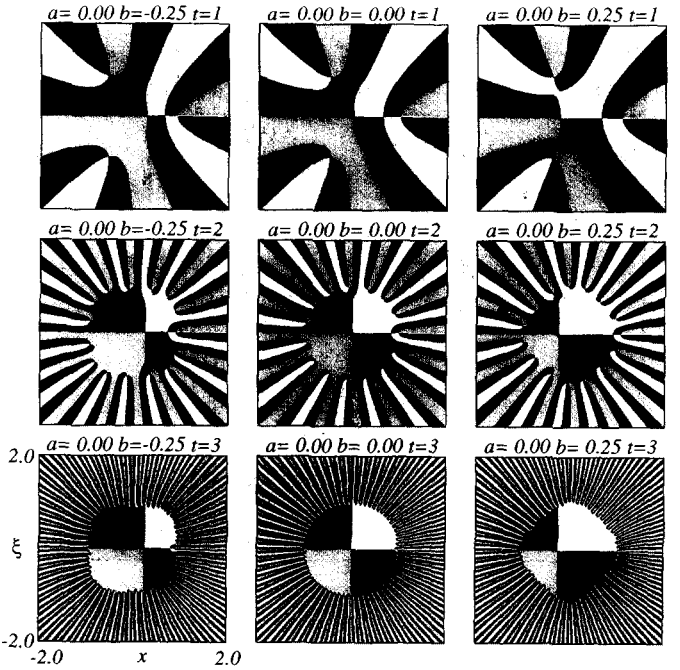
a= 0.00 b=-0.25 t=1
a= 0.00 b= 0.00 t=1
a= 0.00 b= 0.25 t=1
a= 0.00 b=-0.25 t=2
a= 0.00 b= 0.00 t=2
a= 0.00 b= 0.25 t=2
a= 0.00 b=-0.25 t=3
a= 0.00 b= 0.00 t=3
a= 0.00 b= 0.25 t=3
2.0
ξ
-2.0
-2.0
x
2.0

Fig. 4.

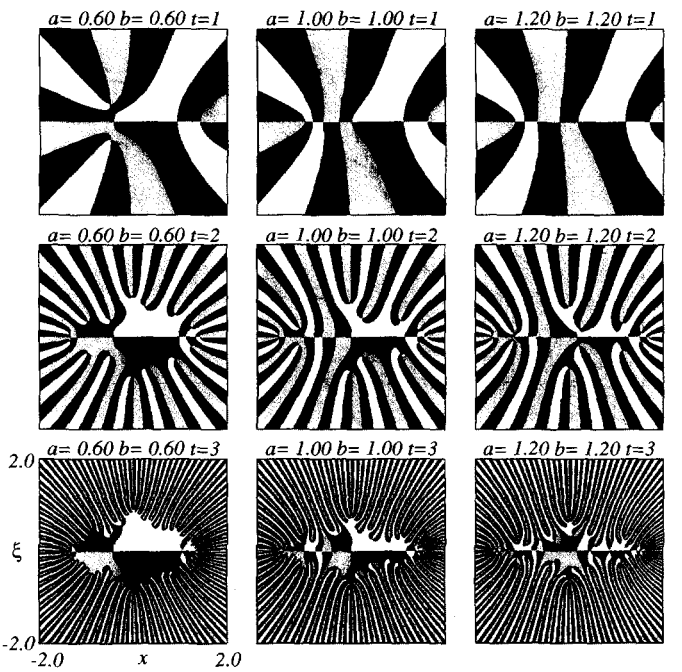
a= 0.60 b= 0.60 t=1
a= 1.00 b= 1.00 t=1
a= 1.20 b= 1.20 t=1
a= 0.60 b= 0.60 t=2
a= 1.00 b= 1.00 t=2
a= 1.20 b= 1.20 t=2
a= 0.60 b= 0.60 t=3
a= 1.00 b= 1.00 t=3
a= 1.20 b= 1.20 t=3
2.0
ξ
-2.0
-2.0
x
2.0

Fig. 5.

from the existence of more then one Riemann sheet supporting different stable dynamics. Since there are two attractors at the tail, there must be now a subdivision of the space of variables into more than the two familiar basins, namely the basin of the attractor at infinity and the basin of the attractor at finite distances. Fig. 6 illustrates typical basins of attraction for parameters in the tail region of every shrimp [1]. In it one sees that although the dynamics in the space of variables is still a period-1 orbit (fixed point), for $3/4 \leq a \leq 1$ we now find two basins corresponding to attractors at finite distances. The remarkable feature of these basins is that although they are still basins of fixed points, they are both *non-homeomorphic to the familiar basin of fixed points displayed for example in Fig. 4.* Further, one recognizes that they are both composed of an infinite collection of totally disconnected domains. As may be recognized by comparing this situation with that depicted in Fig. 1, while non-homeomorphic frontiers imply the occurrence of a bifurcation for unimodal maps, in multimodal maps non-homeomorphic frontiers might also indicate the *existence of more than one stable isoperiodic attractor.* This feature is quite different from all those known for unimodal maps and indicates an alternative origin for "sensitivity on initial conditions".

7. What are generic invariant manifolds made of?

We now argue through an example that the same type of frontiers discussed for the quadratic map also applies to all dynamical systems of higher dimensionality. This unification is important because the current literature on the subject [13,16], implicitly or not, still separates "complex analytic dynamics" from "real dynamics", regarding them as two different subjects that sometimes "share analogous features". As discussed here, real dynamics are in fact *restricted views* on particularly interesting planes, sections from the generalized multidimensional space where the full dynamics lives. As more parameters and variables are considered, the richness of the behavior observed arises primarily from the plethora of possibilities of *combining* collisions of zeros in higher dimensions, not from something else. It is clear that as the dimension of the generalized space increases, its description becomes more and more involved. To illustrate a typical high-dimensional entangling we now discuss briefly the evolution of the zeros of the first iterates of the Hénon map [19–21]

$$x_{t+1} = a - x_t^2 + by_t, \tag{7.1a}$$

$$y_{t+1} = x_t. \tag{7.1b}$$

Fig. 4. Evolution of all zeros of the first three iterates of $x \mapsto (a - x^2)^2 - b$, Eq. (1.4), for parameters close to the period-1 head at $(a, b) = (0, 0)$. The meaning of the colors is explained in Section 2. The scale shown for $a = 0, b = -0.25, t = 3$ is the same for all other values of a, b, t.

Fig. 5. Evolution of all zeros of the first three iterates of $x \mapsto (a - x^2)^2 - b$, Eq. (1.4), for parameters close to the period-1 tail at $(a, b) = (1, 1)$. The meaning of the colors is explained in Section 2. The scale shown for $a = b = 0.6, t = 3$ is the same for all other values of a, b, t.

Although this model looks similar to the two-dimensional model defined in Eq. (4.1), there is a crucial difference: while by construction x_t and ξ_t in Eq. (4.1) must always obey the Cauchy-Riemann conditions, in Eq. (7.1) x_t and y_t are totally free from this constraint. Accordingly, the generalized space corresponding to Eq. (7.1) is eight-dimensional, not four-dimensional as that of Eq. (4.1). Calling η_t the ghost variable associated with y_t we obtain the following four-dimensional cut, characterized by having a and b always real in it:

$$x_{t+1} = a - x_t^2 + by_t + \xi_t^2, \tag{7.2a}$$

$$y_{t+1} = x_t, \tag{7.2b}$$

$$\xi_{t+1} = -2x_t\xi_t + b\eta_t, \tag{7.3a}$$

$$\eta_{t+1} = \xi_t. \tag{7.3b}$$

One recognizes that ξ_t^2 in Eq. (7.2a) and $-2x_t\xi_t$ in (7.3a) provide the coupling between real and ghost variables. Further, that Eq. (7.2a) is totally insensitive to the sign of ξ_t. As previously in Eq. (2.1), Eq. (7.1) also has two fixed points (x_s, x_s) and (x_u, x_u), where now

$$x_s = (-1 + b + \sqrt{(1+b)^2 + 4a})/2, \qquad x_u = (-1 + b - \sqrt{(1+b)^2 + 4a})/2. \tag{7.4}$$

The corresponding interval of stability for (x_s, x_s) is

$$-\tfrac{1}{4}(1-b)^2 \leq a \leq \tfrac{3}{4}(1-b)^2. \tag{7.5}$$

For $b = 0$ the dynamics of the Hénon map reduces to that of two quadratic maps (i.e. remains forever a *two-dimensional* system).

When iterated, Eqs. (7.2) produce a sequence of functions analogous to those obtained for the quadratic map. Eq. (7.2a) produces a family $F_t = F_t(x, y, a, b; \xi)$ while (7.2b) produces $G_t = G_t(x, y, a, b; \xi)$. As already said, these two functions are not connected by the Cauchy-Riemann condition and, consequently, allow a considerably richer dynamics. There are also two additional sequences of functions arising from iterating Eq. (7.3). However, since we want to illustrate the method rather then present an exhaustive discussion of the Hénon map, here we will only present some results obtained for F_t and

---

Fig. 6. Basins of attraction of fixed points of $x \mapsto (a - x^2)^2 - b$ for two sets of parameters along the diagonal $a = b$. Here, the yellow background represents the basin of the fixed point at infinity. For $a = 0.6$ there is only one attracting fixed point, $x \simeq -0.42195444$, with its basin of attraction represented in black. For $a = 1.2$ there are two different attracting fixed points, $x \simeq -1.17082039$ and $x \simeq 0.17082039$ black and purple indicating their respective basins of attraction.

Fig. 7. Evolution of the zeros for some iterates of the Hénon map, Eq. (5.1), as seen on the $x \times y$ cut of the generalized space. The meaning of the colors is explained in Section 2. The scale shown for $a = 1.4, b = 0.3, t = 8$ is the same for all other values of a, b, t.

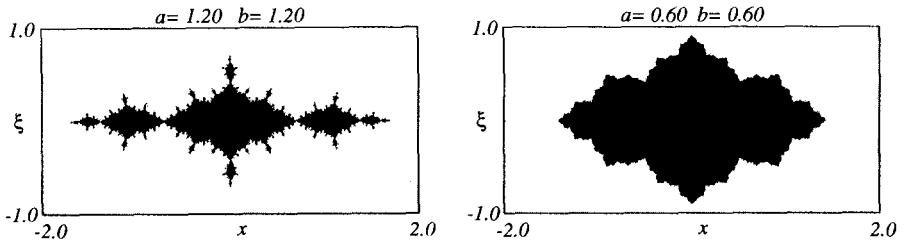
a= 1.20 b= 1.20
a= 0.60 b= 0.60
1.0
-1.0
ξ
-2.0
x
2.0

Fig. 6.

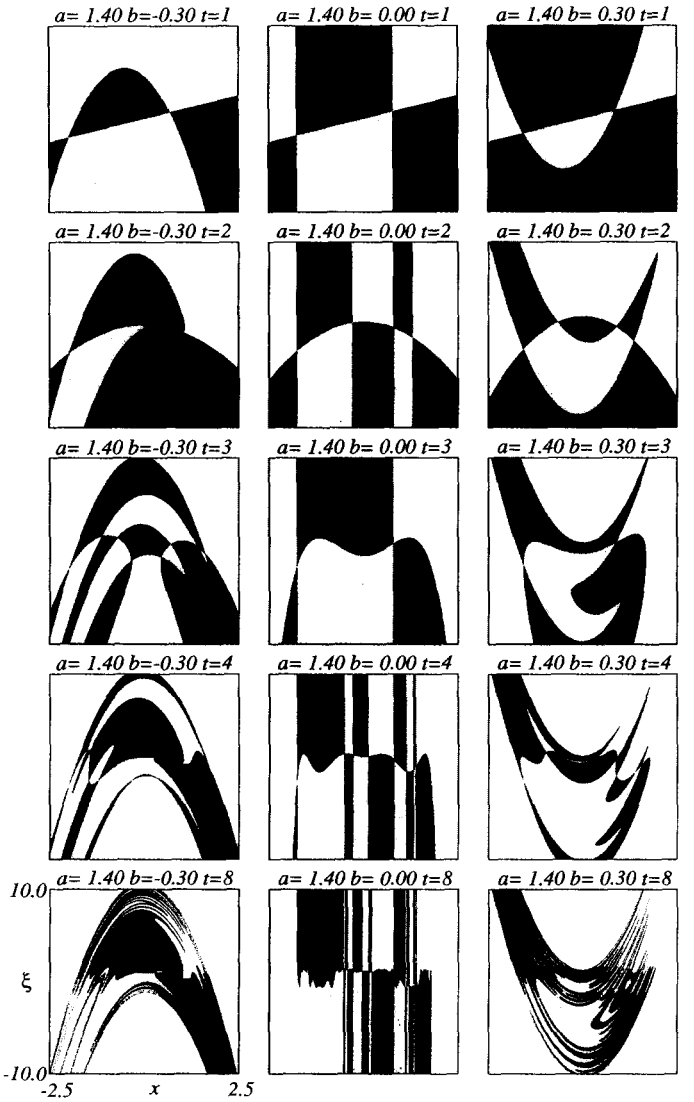
a= 1.40 b=-0.30 t=1
a= 1.40 b= 0.00 t=1
a= 1.40 b= 0.30 t=1
a= 1.40 b=-0.30 t=2
a= 1.40 b= 0.00 t=2
a= 1.40 b= 0.30 t=2
a= 1.40 b=-0.30 t=3
a= 1.40 b= 0.00 t=3
a= 1.40 b= 0.30 t=3
a= 1.40 b=-0.30 t=4
a= 1.40 b= 0.00 t=4
a= 1.40 b= 0.30 t=4
a= 1.40 b=-0.30 t=8
a= 1.40 b= 0.00 t=8
a= 1.40 b= 0.30 t=8
10.0
-10.0
ξ
-2.5
x
2.5

Fig. 7.

G_t as seen on $x_t \times y_t$ cuts for $\xi = 0$. Fig. 7 shows the evolution of the first few generations of zeros for $a = 1.4$, and $b = -0.3, 0.0$ and 0.3. The values $(a, b) = (1.4, 0.3)$ are the same ones discussed by Hénon [19] and many others since then. The center column corresponds to the quadratic map and serves as a reference for comparisons. Although such diagrams display restricted views, one may already identify the portions which belong to the basin of attraction of the stable attractor in each case. We stress that while it is common to refer to the $b = 0$ limit of the Hénon map as "corresponding" to a quadratic map, the Hénon map remains always a two-dimensional map, even for $b = 0$.

8. Conclusions

As seen from the examples above, the introduction of a generalized space allows the investigation of dynamical behaviors to be transformed into an investigation of the topology and properties of the hypersurfaces $U_t = 0$ and $V_t = 0$ generated by the iteration. An interesting observation is the important role played by the set of zeros on this hierarchy of hypersurfaces. These zeros provide a very natural alternative characterization of the well-known F-set, a characterization allowing F-sets to be constructed systematically. By studying the dynamics of the zeros (and their closures) which build basin boundaries (i.e. F-sets) it is possible to realize that under absolute-precision arithmetics, "unstable" orbits are in fact quite "stable" orbits of dynamics confined to the F-set. The essential difference between what is usually referred to as "stable" and "unstable" orbits is that "unstable" orbits can only attract along very particular directions in the configuration-space, directions which are non-dense (in fact, frequently very far from dense). All "instability" frequently attributed to the dynamics on F-sets is nothing else but a consequence of performing computations with finite-precision. Instability does not exist in a strict mathematical sense, when we may pretend to be always able to characterize any given number precisely. For example, $1 + \sqrt{17}$ and $1 - \sqrt{17}$ are irrationals but their sum is not. On the other hand, $\pi = 3.1415\ldots$ and $e = 2.7182\ldots$ have been proven to be transcendental. But what about the nature of $\pi + e$? Which physics should one expect from, say, a multidimensional polynomial map with rational parameters started from initial conditions which are functions, simple or not, of $\pi + e$? As in Section 5, the knowledge of the precise dynamics seems to be deeply connected with the knowledge of numbers and their relative commensurabilities. For suitably chosen parameters, the two-dimensional map $(x, \xi) \mapsto (a + \xi^2 - x^2, -2x\xi)$ allows investigations of the dynamics on F-sets to be performed with absolute numerical precision. By considering a convenient parametrization of all rational numbers living on the unit circle, their dynamics under the map and their commensurability properties with certain transcendental numbers one may identify analytically "sensitivity to initial conditions" as originating from the structural properties of the set of numbers defining parameters and initial conditions (in addition to the requirement of performing all arithmetics with absolute precision). Thanks to the immutable and powerful algebraic closure imposed by the equations of motion, as soon as the "dynamical numbers" (i.e. parameters and initial conditions) are known and fixed

in some particular set of numbers, the definition of the final attractor can be done with no uncertainty. These ideas are elaborated elsewhere [22].

Acknowledgement

The author thanks Professor Celso Grebogi for an invitation to report these results on a Dynamics Pizza Lunch Seminar in College Park, in December of 1993. He also thanks Robert Cawley, Celso Grebogi, Brian Hunt, Arieh Iserles, Edward Ott, Timothy Sauer and James A. Yorke for their kind feedback at that opportunity. Helpful discussions with Phillip Duxbury and Hans Jürgen Herrmann at the HLRZ are gratefully acknowledged. I am also indebted to Bastien Chopard and Peter Ossadnik for kindly sharing their postscript expertise with me.

Appendix A

In this appendix we show that parameter loci corresponding to superstable orbits in phase-space of $x \mapsto (a - x^2)^2 - b$, Eq. (1.4), are *self-inverse* curves. To this end it is enough to study orbits passing through the *critical points* of the map, i.e. through the points where the first derivative of the map is zero. Eq. (1.4) has three critical points: $x = -\sqrt{a}, 0$ and $\sqrt{a}$. Orbits through critical points produce two different sets of equations: the *unique* set $U_t \equiv f_t(x = 0, a, b)$ and the *degenerate* set $D_t \equiv f_t(x = \pm\sqrt{a}, a, b)$, where t denotes the order of the composition. To fix ideas we consider the first two compositions of Eq. (1.4). The arguments, however, are general and apply to all other subsequent compositions as well. The first two compositions going through critical points are

$$U_1 = a^2 - b, \qquad U_2 = [a - (a^2 - b)^2]^2 - b, \tag{A.1}$$

$$D_1 = -b, \qquad D_2 = (a - b^2)^2 - b. \tag{A.2}$$

Critical points inside periodic cells must be periodic too, thereby implying $U_t = 0$ and $D_t = \pm\sqrt{a}$ for all t. This fact yields at once

$$a = \pm\sqrt{b} \quad \Leftrightarrow \quad \pm\sqrt{a} = -b,$$

$$a - (a^2 - b)^2 = \pm\sqrt{b} \quad \Leftrightarrow \quad \pm\sqrt{a} = (a - b^2)^2 - b,$$

and similar equations for higher-order compositions, demonstrating the self-inverse nature of all superstable loci. Studying U_t and D_t it is possible to recognize other interesting properties of superstable loci recurring within each t–periodic cell, for example: (a) superstable loci are central projections of circles, e.g. each period-1 locus is a shadow cast on the horizontal $a \times b$ plane by a light source located at the same level of the uppermost point of a circle perpendicular to the plane; (b) the effect of increasing the periodicity is to translate and rotate the circles; (c) from U_t and D_t one may extract

determinants Δ_t allowing the investigation of the particular set of numbers (parameters) selected by the dynamics of the zeros of the derivative of the map. For example, all crossings of period-2 superstable loci in parameter space are contained among the roots of the discriminant of an 8×8 matrix:

$$\begin{aligned}\Delta_2 = {} & a^4(a-1)^2[1+a+a^2]^2(1+2a^2-3a^3+3a^4-3a^5+a^6) \\ & \times(1-39a^3+37a^6-11a^9+a^{12})(1+a^3+9a^6-7a^9+a^{12}) \\ & \times(1+a^3+a^6-3a^9+a^{12}) \\ & \times[1-2a^2-6a^3+a^4+9a^5+5a^6-3a^7-2a^8+3a^9+6a^{10}+3a^{11}+a^{12}];\end{aligned}$$

(d) Δ_3 is the determinant of a 48×48 matrix; (e) the location of intersections of superstable loci corresponding to orbits of *any arbitrary periodicity* are given by similar determinants.

These and some other consequences of the great symmetry among all U_t and D_t will be discussed elsewhere.

References

[1] J.A.C. Gallas, (a) Physica A 202 (1994) 223; (b) Phys. Rev. E 48 (1993) R4159; (c) Preprint HLRZ 66/93.
[2] O. Neugebauer, The Exact Sciences in Antiquity (Princeton University Press, 1952, reprinted by Dover, NY, 1969).
[3] F. Klein, 1894 Easter lectures at the University of Göttingen, published as Vorträge über Ausgewählte Fragen der Elementargeometrie, 1895; English translation: Famous Problems of Elementary Geometry (reprinted by Dover, NY, 1956).
[4] (a) E. Schröder, Math. Ann. 2 (1870) 317–365; 3 (1871) 296–322;
(b) B. Derrida, A. Gervois and Y. Pomeau, J. Phys. A 12 (1979) 269–296;
(c) P. Collet and J.P. Eckmann, Iterated Maps on the Interval as Dynamical Systems (Birkhäuser, Basel, 1980);
(d) S. Chang, M. Wortis and J.A. Wright, Phys. Rev. A 24 (1981) 2684;
(e) L. Glass and R. Perez, Phys. Rev. Lett. 48 (1982) 1772–1775;
(f) L. Glass, Chaos 1 (1991) 13–19.
[5] P. Fatou, C. R. Acad. Sci. 143 (1906) 546–548.
[6] P. Fatou, C. R. Acad. Sci. 164 (1917) 806–808.
[7] P. Fatou, C. R. Acad. Sci. 165 (1917) 992–995.
[8] P. Montel, (a) C. R. Acad. Sci. 153 (1911) 996–998, 1455–1456; (b) Ann. Écol. Norm. Sup. 33 (1916) 223–302; (c) Leçons sur les famillies normales de fonctions analytiques et leurs applications (Gauthier-Villars, Paris, 1927).
[9] H. Brolin, Arkiv för Mathematik 6 (1965) 103–144.
[10] M.V. Jakobson, Math. USSR Sbornik 6 (1968) 97–114.
[11] M.K. Oba and T.S. Pitcher, Trans. Am. Math. Soc. 166 (1972) 297–308.
[12] P. Blanchard, Bull. Am. Math. Soc. 11 (1984) 85–141.
[13] R.L. Devaney, An Introduction to Chaotic Dynamical Systems, second edition (Addison-Wesley, Redwood City, 1989).
[14] A.F. Beardon, Iteration of Rational Functions (Springer Verlag, NY, 1991).
[15] D. Gulik, Encounters with Chaos (McGraw-Hill, NY, 1992).
[16] N. Steinmetz, Rational Iteration (Walter de Gruyter, Berlin, 1993).
[17] P. Fatou, Bull. Soc. Math. Fr. (a) 47 (1919) 161–271; (b) 48 (1920) 33–94; (c) 48 (1920) 208–314.
[18] G. Julia, J. Math. Pures et Appl. 4 (1918) 47–245.

[19] M. Hénon, Commun. Math. Phys. 50 (1976) 69–77.
[20] J.A.C. Gallas, Phys. Rev. Lett. 70 (1993) 2714–2717.
[21] L. Mora and M. Viana, Acta Math. 171 (1993) 1–71.
[22] J.A.C. Gallas, preprint HLRZ 01/94.